Journal of Molecular Liquids 437 (2025) 128412

Contents lists available at ScienceDirect

Journal of Molecular Liquids

journal homepage: www.elsevier.com/locate/molliq

Beyond the blend: Unveiling the thermophysical fingerprints of hydrated choline chloride deep eutectic systems with bio-derived and synthetic hydrogen bond donors

Rafael Alcalde [a], Sergio de-la-Huerta-Sainz [a], Valentin Diez-Cabanes [a], María A. Escobedo-Monge [a], Jose.L. Trenzado [b], Mert Atilhan [c], Alfredo Bol [d,e], Santiago Aparicio [a,e,*]

[a] Department of Chemistry, University of Burgos, 09001 Burgos, Spain
[b] Department of Physics, University of Las Palmas de Gran Canaria, 35017, Las Palmas G.C., Spain
[c] Department of Chemical and Paper Engineering, Western Michigan University, Kalamazoo, MI 49008-5462, USA
[d] Department of Physics, University of Burgos, 09001 Burgos, Spain
[e] International Research Center in Critical Raw Materials for Advanced Industrial Technologies (ICCRAM), University of Burgos, 09001 Burgos, Spain

ARTICLE INFO

Keywords:
Deep eutectic solvents
Thermophysical properties
Choline chloride
Hydration effects
Bio-based hydrogen bond donors

ABSTRACT

This study presents a comprehensive thermophysical characterization of hydrated deep eutectic solvents (DESs) composed of choline chloride (ChCl) and four hydrogen bond donors (HBDs): citric acid, malic acid, fructose, and ethylene glycol in equimolar ratios. By introducing 2, 10, and 22 wt% water—spanning key hydration regimes where DESs structure is progressively altered—we systematically quantify the effects of hydration on density, viscosity, electrical conductivity, thermal conductivity, and refractive index over a wide temperature range. Results demonstrate that water addition leads to a dramatic reduction in viscosity, particularly for bio-derived HBDs, enhancing processability and enabling practical applications. The ChCl:citric acid DESs maintains high structural cohesion upon hydration, reflected in persistent cooperative dynamics and high activation energy, whereas the synthetic ethylene glycol system exhibits predictable, tunable behavior, ideal for engineered fluid systems. Electrical conductivity increases non-linearly with water content, accompanied by a transition from fragile to strong liquid behavior. Derived parameters—molecular volume, thermal expansion coefficient, and excess molar volumes—reveal non-ideal mixing behavior and structural reorganization. Our findings define structure–property correlations critical for optimizing DESs formulations, offering a foundation for application-specific solvent engineering in energy, electrochemistry, and separation technologies.

1. Introduction

The need for more sustainable, environmentally friendly and safer (green) solvents [1] to replace traditional ones [2], has led to the extensive research on Deep Eutectic Solvents (DESs) [3] considering their advantages over common Volatile Organic Compounds (VOCs) frequently used in the industry as solvents [4], such as biodegradability and low volatility. Nevertheless, it should be remarked that not all the possible or considered DESs are biodegradable or may be considered as green or sustainable [5], thus being largely dependent on the nature and origin of the molecules considered for DESs development, which need to be carefully considered in terms of DESs properties, safety and sustainability [6].

DESs are formed through the suitable combination of two or more compounds [7], which results in the formation of strong intermolecular hydrogen bonds [8]. These interactions lead to melting point depression in comparison with ideal liquid mixture behavior, used to assure the formation of a true DES [9], [10], and thus, some authors [11] have proposed the term Low Melting Mixtures (LMMs) [12]. Nevertheless, the term DESs will be maintained in this work in agreement with most of the available literature in this area.

DESs can be classified into five main categories (type I to type V [13], [14]), depending on the nature of the forming compounds. Among them, type III ones, usually containing at least an ionic compound have

* Corresponding author at: Department of Chemistry, University of Burgos, 09001 Burgos, Spain.
E-mail address: sapar@ubu.es (S. Aparicio).

https://doi.org/10.1016/j.molliq.2025.128412
Received 29 May 2025; Received in revised form 25 August 2025; Accepted 26 August 2025
Available online 27 August 2025

attracted great attention, being typically developed by mixing a quaternary ammonium salt, such as commonly choline chloride (CC), along with a hydrogen bond donor (HBD), such as organic acids, polyols, or sugars [15]. Of particular interest are those DESs based on naturally – based compounds [16], like citric acid (CA), malic acid (MA), and fructose (FR), combined with non-toxic salts like CC, leading to the formation of type III Natural DESs (i.e. NADESs). These components are non-toxic and renewable, making them valuable choices for various applications in fields such as pharmaceuticals, foods, electrochemistry, and biomass processing [17], [18], [19]. Relevant DESs may also be obtained through the combination of CC with molecules such as ethylene glycol (EG), showing suitable physicochemical properties. These compounds (CC + {CA, MA, FR, EG}) are considering specifically:

- CA and MA are polycarboxylic organic acids with multiple functional groups, offering high hydrogen bonding capacity and bio-derived origin.
- FR is a sugar-type HBD with extensive hydroxyl functionality and rigid molecular architecture, providing a model for complex, naturally occurring systems.
- EG is a simple synthetic polyol often used in benchmark DESs studies, providing a comparison to more flexible and industrially common systems.

This selection allows to examine how molecular complexity, hydrogen bonding site density, and bio-based vs. synthetic origin influence DESs behavior upon hydration. The combination covers a representative spectrum of natural and synthetic HBDs to derive structure–property insights applicable to a broad range of DESs formulations.

Another relevant classification for DESs / NADESs stands on their hydrophobic or hydrophilic nature [20], [21]. The presence of water in any considered DESs / NADESs may largely affect their physicochemical properties even for hydrophobic ones [22]. The use of DESs / NADESs for industrial / technological applications may lead to water absorption from the environment, which would lead to relevant modifications in solvent properties, especially for hydrophilic type III DESs / NADESs. The suitability of water molecules for developing strong hydrogen bonding with DESs / NADESs components, may lead to disruption / modification of the hydrogen bonding among molecules forming the DESs [23], thus changing their macroscopic behavior and properties [24]. Likewise, the addition of water to DESs may also lead to benefits, e.g. water content can be use for controlling and fine tuning DESs viscosity [25], which for many DESs is remarkably high and may lead to scaling up problems because of hindering heat and/or mass transfer operations [26]. Likewise, for type III DESs / NADESs, i.e. those containing ionic species such as CC, the water content may be used for controlling solvent electrical conductivity [27], which is pivotal for possible electrochemical applications.

The effect of water on DESs / NADESs properties is largely dependent on water content [28], with three well defined regions [29] for most of the DESs in which: *i*) DESs microstructuring and properties are maintained (usually water content lower than 10 wt%), *ii*) transition region in which DESs hydrogen bonding start to evolve disrupting their hydrogen bonding network (usually water content lower than 30 wt%), and *iii*) solution of DESs component dispersed into water prevailing environment (usually water content higher than 30 wt%). Therefore, to analyze the mechanism(s) water – DESs / NADESs interactions, as well as how it affects the macroscopic thermophysical properties is crucial for DESs / NADESs effective design and application.

Despite the growing interest in hydrated DESs, comprehensive studies that systematically correlate water content with molecular dynamics, structure–property relationships, and application-relevant performance across multiple HBD chemistries remain scarce. In particular, comparative insights between synthetic and bio-based hydrogen bond donors under controlled hydration have not been fully explored. This work addresses that gap by integrating experimental measurements with thermodynamic modeling across four choline chloride-based DESs systems (citric acid, malic acid, fructose, ethylene glycol), each evaluated at three distinct hydration levels. The use of Vogel–Fulcher–Tammann (VFT) analysis, combined with derived descriptors such as fragility, activation energy, and excess molar volume, enables a deeper understanding of how water modulates cooperative dynamics and ionic transport. Furthermore, by benchmarking the fluid properties against industrial targets, we provide a practical framework for tailoring DESs formulations via hydration for real-world applications in electrochemistry, separation, and thermal systems.

Previous research has shown that adding water typically remarkably lowers viscosity and density while increasing electrical conductivity and diffusivity [30]. However, how much these properties change depends on the specific compounds used for DESs formation used and the amount of water added. For example, DESs comprising carboxylic acids are particularly sensitive to hydration [24]. Additionally, thermodynamic properties of water – DESs mixtures, such as excess molar volumes and expansion coefficients upon mixing [31], [32], have showed largely non-ideal behavior resulting on the development of water – DESs hydrogen bonding disrupting the internal DESs intermolecular interactions. Nevertheless, there are scarce literature studies that comprehensively compare various DESs systems at controlled hydration levels.

A systematic investigation into how water content affects key properties across a range of natural compound – based NADESs is still lacking. The study reported in this work aims to address these gaps by exploring how water modifies the thermophysical properties of four different CC-based DESs using CA, MA, FR and EG, all prepared in a 1:1 ratio, Fig. 1. All DESs in this study were prepared using a 1:1 mole ratio of CC to each HBD. This choice aligns with previous literature reports where such ratios are commonly used, particularly in the formulation of Natural Deep Eutectic Solvents (NADES) involving bio-derived compounds [33]. While thermodynamically rigorous eutectic compositions may differ from these ratios—as demonstrated, for example, in the case of CC:EG by Hayler and Perkin [34]—the 1:1 mixtures are known to form stable liquids at room temperature, enabling consistent comparative analysis across different HBD types. Moreover, 1:1 ratios facilitate balanced hydrogen bonding interactions and are often favored for optimizing physicochemical properties such as viscosity and conductivity in practical applications.

This research takes an integrated approach, analyzing a wide range of properties, including density, viscosity, electrical and thermal conductivity, and how these evolve in wide temperature ranges. The analysis of these properties uncovers the structure of hydrated NADESs systems, especially focusing on the differences between synthetic hydrogen bonding compounds (EG) and natural ones (CA, MA, FR). This understanding allows their use for real-world environments that contain water and can be used to tailor DESs / NADESs operations in various sectors including energy storage and pharmaceuticals via hydration, for developing DES/NADES-based next-generation solvents.

2. Methods

2.1. Chemicals and DESs preparation

The characteristics of the chemicals used for DESs preparation are reported in Table 1, these chemicals were used as received from the supplier without additional purification. DESs for CC + {CA, MA, FR or EG} were all prepared for 1:1 mole ratios by weighing (Mettler AT261 balance, $\pm$ 1 10^{-5} g) suitable amounts of each component, mixtures were heated (60 °C) under stirring for 24 h, with the formation of the corresponding transparent liquid phases. Liquid samples were stored at ambient conditions in sealed bottles in darkness, do not show alteration 30 days after their preparation. All DESs considered in this study (ChCl: HBD at 1:1 mole ratio) were prepared following standard protocols widely reported in the literature [33], [35]. The resulting liquids were

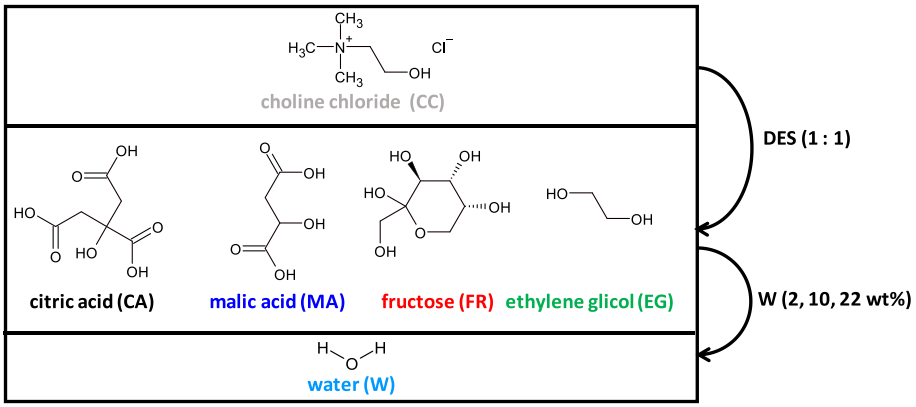

Fig. 1. Molecules considered in this work for the DESS formation and preparation of mixtures with water.

Table 1
Chemicals used in this work for experimental studies.

chemical	formula	molar mass / g mol^{-1}	purity / %	CAS - number	source
CC	$C_5H_{11}N_2O_2$	117.15	99.0	107–43-7	Sigma-Aldrich
EG	$C_2H_6O_2$	62.07	99.8	107–21-1	Sigma-Aldrich
CA	$C_6H_8O_7$	192.12	99.5	77–92-9	Sigma-Aldrich
MA	$C_4H_6O_5$	134.09	99.0	6915-15-7	Sigma-Aldrich
FR	$C_6H_8O_7$	192.12	99.8	77–95-9	Sigma-Aldrich
water	H_2O	18.02	resistivity at 298.15 K = 18.2 MΩ cm	7732-18-5	Milli-Q (Millipore)

homogeneous, transparent, and stable over at least 30 days. No further molecular-level spectroscopic characterization (e.g., FT-IR, ^{1}H NMR) was performed, as the identity and liquid-state behavior of these DESs have been extensively validated in previous work. This study focuses instead on their macroscopic thermophysical properties under controlled hydration conditions. To account for any residual moisture present in the raw materials or captured during the preparation process, the initial water content in the freshly prepared neat DESs (i.e., without added water) was quantified using Karl-Fischer coulometric titration (Metrohm 831 KF, ± 0.3 %). The measured values were: 0.25, 0.12, 0.11 and 0.06 water wt%, for DESs containing FR, MA, EG, and CA, respectively. This intrinsic water content was included in the total hydration calculations when preparing the DESs + water mixtures by weighing for 2, 10 and 22 wt% water content. Therefore, all reported water contents reflect the true total water content in the system, ensuring consistency across the measured samples. Samples were kept in sealed bottles to avoid absorption of additional atmospheric water.

2.2. Apparatus and procedures

All experimental studies were carried out at atmospheric pressure. The experimental density data, ρ, ($\pm$ 1•10^{-4} g cm^{-3}) data for liquid mixtures of CC + {CA, MA, FR or EG} in 1:1 ratio with different percentage of water (10 or 22 wt%) at different temperatures were measured using an Anton Paar DMA1001 vibrating tube densimeter, with cell temperature controlled and measured with an internal peltier to ±0.01 K. The densimeter was calibrated using water (ISO-17034 certified material) and air as reference fluids, fulfilling ISO-5725. From these ρ data, the thermal expansion coefficient, α_p, for each mixture was calculated from linear fits of ρ vs temperature ($R^2 > 0.9999$) according to Eq. (1):

$$\alpha_p = -\frac{1}{\rho}\left(\frac{\partial\rho}{\partial T}\right)_p \quad (1).$$

Dynamic viscosities, η, were measured using an electromagnetic VINCI Tech. EV1000 electromagnetic piston moving viscometer, the cell temperature was controlled with a Julabo Presto circulating bath and measured with platinum resistance thermometers (PRT) inside the measuring cell (± 2 % uncertainty for viscosity and ± 0.01 K for temperature). Prior to the measurements, the viscometer was calibrated using certified oils provided by the manufacturer. Viscosity measurements were carried out in a continuous sweeping mode, in which the cell temperature is changed at 5 °C per hour and viscosity is registered continuously. In this way, the whole viscosity–temperature curve at isobaric conditions is recorded instead of measuring viscosity at selected fixed temperatures. Temperature dependence of viscosity cannot be adequately described by the Arrhenius equation, and thus it was fitted considering the Vogel–Fulcher–Tammann equation (VFT):

$$\eta = Ae^{\frac{B}{T-T_0}} \quad (2)$$

The Angell's fragility coefficient, D_f, is calculated as:

$$D_f = \frac{B}{T_0} \quad (3)$$

From which the activation energy of the viscous flow, E_η, was calculated:

$$E_\eta = R\left[\frac{B}{\frac{T_0^2}{T^2} - \frac{2T_0}{T} + 1}\right] \quad (4)$$

where R is the molar gas constant, 8.314 J·mol^{-1} K^{-1}; B and T_0 represents adjustable parameters of the equation VFT and T is the absolute temperature.

Refraction index was measured with regard to sodium D-line (n_D, uncertainty ±1 10^{-5}) with a Leica AR600 refractometer with the cell temperature controlled with an external circulator (Julabo F32) and measured with a PRT (± 0.01 K). Refraction index allowed the calculation of molar refraction, R_m, and polarizability, α, as follows:

$$R_m = \left(\frac{n_D^2 - 1}{n_D^2 + 2}\right)V_m \quad (5)$$

$$\alpha = \frac{3\,R_m}{4\,\pi\,N_A} \quad (6)$$

where V_m stands for the mixture molar volume.

Electrical conductivity, σ, was measured with a VWR pHenomenal conductivity meter, and the cell temperature was controlled by a Julabo

F25 circulating bath and measured in situ with platinum resistance thermometers (± 0.01 K). The conductivity meter was calibrated with standard KCl solutions (± 0.5 % uncertainty). Thermal conductivity, κ, (5 % uncertainty) was measured with a Decagon devices KD2 Thermal analyzer, equipped with a KS-1 sensor (6 cm long, 1.3 mm diameter single needle) with the cell temperature controlled using a Julabo F32 bath and measured with a PRT (± 0.01 K).

The data for the measured thermophysical properties are reported in the Supplementary Information (Tables S2 to S7).

3. Results and discussion

3.1. Thermodynamic analysis of viscous flow and molecular dynamics

The viscosity of DESs + water systems were measured at 2, 10 and 22 wt% water content. Water contents of 2 wt%, 10 wt%, and 22 wt% were selected to represent three regimes of water–DESs interaction. The 2 wt% level corresponds to minimal hydration with preserved DESs structure; 10 wt% represents a transition region where partial network disruption begins; and 22 wt% was chosen to remain below the threshold (~30 wt%) beyond which the system no longer behaves as a DESs but rather as a conventional aqueous solution. This upper limit was selected to probe the maximal effects of hydration while retaining DESs character. In the case of CC:CA DESs it was not possible to measure viscosity at water 2 wt%, neither the other considered thermophysical properties, because of the extremely viscous behavior of the considered system. Based on visual and handling observations, the 2 wt% hydrated CC:CA mixture displayed paste-like, highly viscous behavior, resisting flow even at elevated temperatures (~333 K). Although the viscosity exceeded the measurable limit of our viscometer (>10,000 mPa·s), we estimate it to lie within the range of 10^4–10^5 mPa·s for the 298 to 348 K range. This extreme viscosity precluded reliable measurements but qualitatively confirms the substantial impact of minimal hydration on this system's flow properties.

The viscosity ordering is CA > MA > FR > EG. The DESs with the considered natural compounds (CA, MA and FR) are extremely viscous with low water content, and so in the corresponding neat DESs, which may hinder their possible industrial use and scaling up. Nevertheless, increasing water content up to 22 wt%, in which DESs maintain their nature, and increasing temperature roughly above 320 K, leads to reasonably low viscosity. In the case of DESs containing EG, a low viscous fluid is inferred even for low water content. The viscometric data analyzed through the VFT equation (as non-Arrhenius behavior is inferred for all the considered DESs + water mixtures in the studied temperature range) provides insights into the thermodynamic nature of molecular rearrangements in these aqueous DESs systems, Figs. 2 and S1 (Supplementary Information). The corresponding VFT parameters (Table 2) reveal distinct activation mechanisms of flow, which reflect the underlying potential energy landscape and cooperative molecular motions. In the case of systems with MA and FR for water 2 wt%, as inferred from the χ^2, as well as the corresponding VFT parameters (Table 2) suggest a transition in the viscous flow mechanism, indicating a crossover from cooperative α-relaxation (where multiple molecules move together) to more localized β-relaxation processes. This behavior indicates that the introduction of water disrupts the three-dimensional hydrogen bonding network of CC:MA / FR without providing sufficient hydration to establish new stable configurations. This effect would be even more relevant for CA molecule, with its three carboxyl groups arranged in a specific geometric configuration, likely creates topological constraints that resist the initial stages of water interaction and integration into the corresponding hydrogen bonding network. The B parameter in the VFT equation represents the activation energy and reflects the strength of intermolecular cooperativity. The systematic evolution of B values across water concentrations reveals the progressive deconstruction of the original DESs structure. For CC:CA, the high B values (2521.90 K at 10 wt% and 2401.92 K at 22 wt%) indicate retention of strong cooperative interactions even at high water content, suggesting that water molecules are incorporated into the existing hydrogen bonding framework rather than disrupting it completely. This behavior contrasts with typical molecular solvents where water addition leads to more dramatic reductions in activation energies. This effect is also present in systems with MA / FR and in minor extension in those with EG. The VFT - T_o parameter represents the Vogel temperature, below which cooperative motion would theoretically cease. The evolution of T_o values provides insights into the glass transition behavior and the fragility of these systems. The CC:EG system shows relatively stable T_o values (118.43–143.53 K), indicating that water addition preserves the fundamental relaxation mechanisms while simply modifying their kinetics. Conversely, the CC:CA system exhibits more variable T_o values

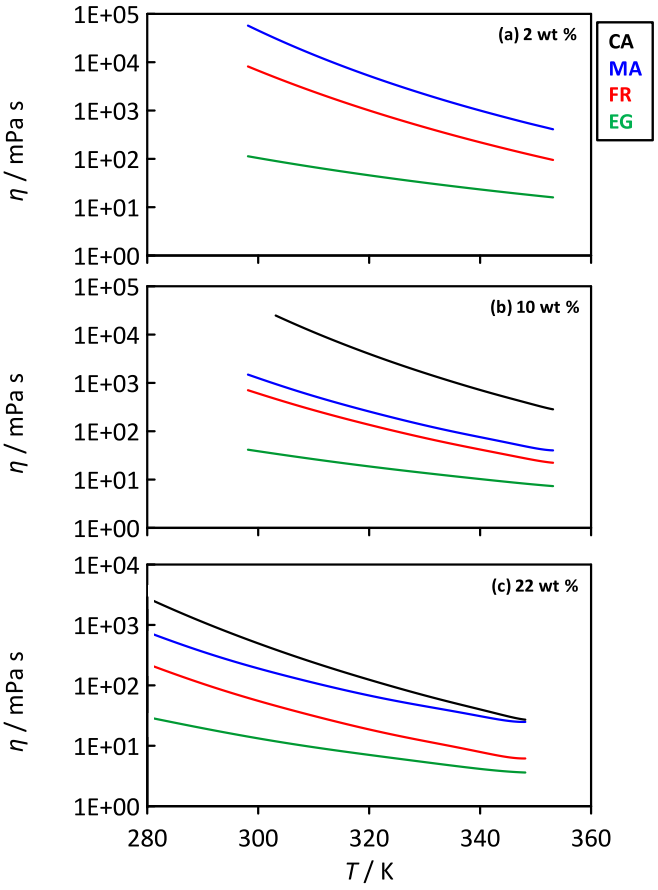

Fig. 2. Dynamic viscosity, η, as a function of temperature, T, for CC:{CA, MA, FR, EG} 1:1 DESS with different water content (indicated as water wt% in each panel).

Table 2
Fitting parameters of experimental viscosity, η, to VFT equation (eq. (2)) for the reported NADESs with variable water content.

System	A / mPa s	B / K	T_o / K	χ^2
(CC:CA) + 2 wt% water	–	–	–	–
(CC:MA) + 2 wt% water	0.0041200	2109.99	169.86	301.0
(CC:FR) + 2 wt% water	0.0002869	2693.45	141.24	161.4
(CC:EG) + 2 wt% water	0.0262164	1504.30	118.43	0.0
(CC:CA) + 10 wt% water	0.0006700	2521.90	158.33	625.9
(CC:MA) + 10 wt% water	0.0059700	1643.10	165.94	90.6
(CC:FR) + 10 wt% water	0.0016800	1937.75	148.53	7.0
(CC:EG) + 10 wt% water	0.0243634	1337.10	118.73	0.0
(CC:CA) + 22 wt% water	0.0006462	2401.92	122.72	50.5
(CC:MA) + 22 wt% water	0.0761500	1037.69	167.39	2.2
(CC:FR) + 22 wt% water	0.0046300	1439.52	146.68	1.1
(CC:EG) + 22 wt% water	0.0479679	879.72	143.53	0.0

across the studied water content range, suggesting water-induced changes in the nature of the cooperative relaxation processes with increasing water content, which would result in the large decrease of viscosity for CA systems both with increasing water content and temperature. Systems with MA / FR shows similar behavior to that for CA. While thermogravimetric analysis (TGA) is a standard method for assessing thermal stability, the present study focuses on a temperature range (typically below <350 K) that is well below the expected decomposition thresholds for all DESs components used. Within this range, no visual degradation, phase separation, or irreversible changes were observed during prolonged measurements. Furthermore, the consistency of the viscosity data across increasing temperatures, along with the VFT results, with high VFT-derived activation energies (B values), and stable Vogel temperatures (T_o), support the conclusion that these systems remain structurally stable under the studied conditions. The absence of anomalies or discontinuities in viscosity and transport properties further confirms the lack of thermally induced degradation. These converging results provide indirect yet robust evidence of thermal stability in the relevant temperature regime, making additional TGA data non-essential for the scope of this investigation.

3.2. Fragility analysis and energy landscape topology

The fragility parameter D_f quantifies the deviation from Arrhenius behavior and provides insights into the cooperativity of molecular motions and the heterogeneity of the energy landscape. Strong liquids (low fragility) exhibit nearly temperature-independent activation energies, while fragile liquids show strong temperature dependence reflecting heterogeneous environments and cooperative rearrangements. The general decrease in fragility with increasing water content (Fig. 3a) across most systems (with the exception of CA-systems) indicates a transition from fragile to more strong-like behavior. This transformation suggests that water addition reduces the heterogeneity of the local environments and smooths the potential energy landscape. From a molecular perspective, this can be interpreted as water molecules filling in the "rough" regions of the energy landscape, providing more uniform pathways for molecular rearrangement. The E_η trends complement the fragility analysis, thus reflecting modifications in the potential energy barriers for molecular motion. For (most) systems showing decreasing E_η with increasing water content, the water molecules are effectively plasticizing the system by providing alternative, lower-energy pathways for molecular rearrangement. This is particularly evident in the CC:EG system, where the simple diol structure allows water molecules to integrate seamlessly into the hydrogen bonding network.

3.3. Ionic transport mechanisms and charge carrier dynamics

The electrical conductivity data, Fig. 4a, show remarkable differences among the considered systems, with the ordering CA < MA < FR being remarkably lower than those for EG. Therefore, the large viscosity inferred for those NADESs with CA / MA / FR leads to low electrical conductivity, largely changed (improved) upon water addition and heating. The analysis of electric conductivity in conjunction with viscosity through the Walden plot, Fig. 4b, reveals the complex relationship between ionic mobility and bulk transport properties. The deviation from the ideal Walden rule (represented by the KCl reference line) quantifies the degree of ionic association [36], Fig. 4c, and the coupling between ionic and molecular motions. Systems lying below the ideal Walden line exhibit subionic behavior, indicating either ion pairing, ionic clustering, or preferential solvation effects that reduce ionic mobility relative to what would be expected from bulk viscosity alone. The CC:CA system consistently shows the largest deviations from ideality, suggesting strong ion-solvent interactions mediated by the multiple functional groups of citric acid. These interactions can be considered

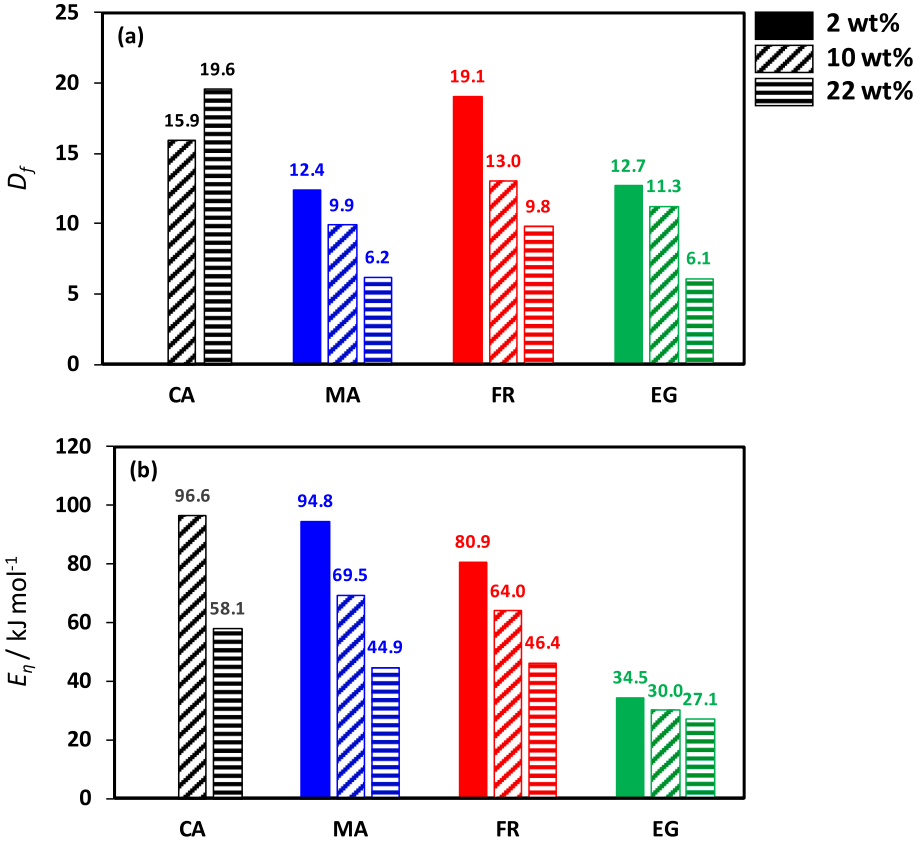

Fig. 3. CC:{CA, MA, FR, EG} 1:1 DESs with different water content reporting (a) Angell's fragility parameter, D_f, and (b) activation energy of the viscous flow, E_η, as obtained from viscosity vs temperature experimental data for the reported DESs as a function of water content.

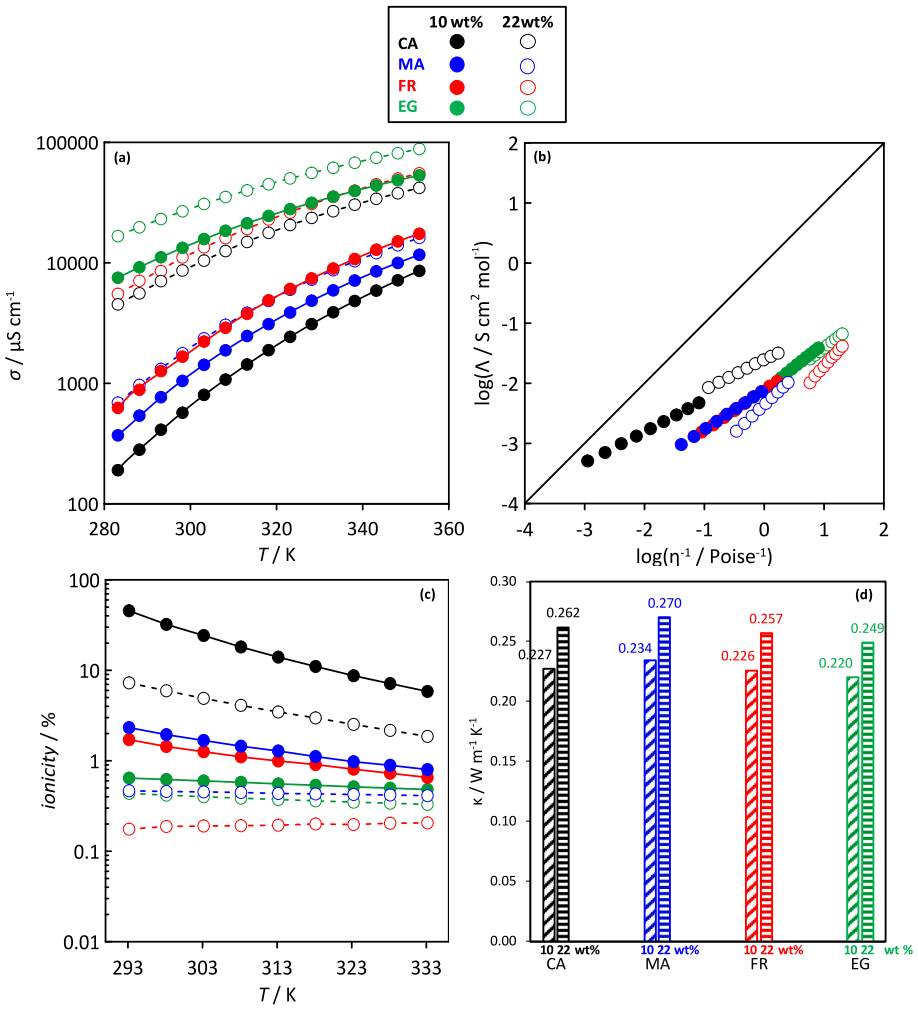

Fig. 4. CC:{CA, MA, FR, EG} 1:1 DESs with different water content reporting (a) electrical conductivity, σ, (b) Walden plot showing fluidity (η^{-1}, where η stands for dynamic viscosity) vs. molar conductivity (Λ) in log–log plot, with diagonal line showing the behavior of KCl 0.01 M reference, (c) calculated percentage of ionicity and (d) thermal conductivity, κ. Values in panel d are reported at 298.15 K.

in terms of preferential solvation shells where the citric acid molecules coordinate more strongly with the chloride anions than with water molecules, creating kinetically distinct ionic environments. The calculated ionicity percentages, Fig. 4c, provide a quantitative measure of the fraction of charge carriers that contribute to ionic conduction. The increase in ionicity with water content reflects the progressive dissociation of ion pairs and the breakup of ionic aggregates. However, the non-linear relationship between water content and ionicity suggests that water molecules are not uniformly distributed but rather organize into specific solvation structures around the ionic species.

Additionally, the thermal conductivity was measured, Fig. 4d, providing additional insights into the transport properties by revealing how energy transfer occurs at the molecular level. The observed increases in thermal conductivity with water addition reflect not only the higher intrinsic thermal conductivity of water but also changes in the phonon transport mechanisms. The formation of hydrogen-bonded water networks can create additional pathways for vibrational energy transfer, leading to enhanced thermal transport properties. Although the measured thermal conductivity data carry an experimental uncertainty of up to ±5 %, the observed increases with water addition are systematic and exceed this margin; e.g. in the transition from 10 wt% to 22 wt% water content this property increase roughly a 15 %. Therefore, while absolute values should be interpreted with caution, the overall trends and relative differences are robust. These results consistently support the interpretation that water integration enhances thermal transport via the formation of extended hydrogen-bonded networks.

3.4. Thermodynamic properties and molecular organization

The density measurements, Fig. 5a, reveal the interplay between molecular packing efficiency and intermolecular interactions. The observed decreases in density with water addition, considering that all the studied DESs are largely hydrophilic and thus showing larger densities than water in the neat state (especially for those containing natural compounds), is firstly produced by the lower molecular weight of water compared to the organic components, but the non-linear relationships with water content suggest structural reorganization effects. The α_p values, Fig. 5b, reflect changes in intermolecular potential energy with temperature. The observed variations in α_p with water content indicate modifications in the anharmonicity of the intermolecular potential wells. Systems with higher α_p suggest looser molecular packing and greater sensitivity to thermal energy, which correlates with the observed viscosity behaviors Fig. 2. This behavior is confirmed by the trends in R_m, Fig. 5c. The excluded volume calculations, Fig. 5d, which are based on hard sphere models, provide insights into the effective molecular sizes and packing efficiencies in these systems. The trends observed suggest that water addition initially improves packing efficiency at low concentrations through better space filling, but leads to increased free volume at higher concentrations as the original DESs structure becomes progressively disrupted. This interpretation agrees with the concept of

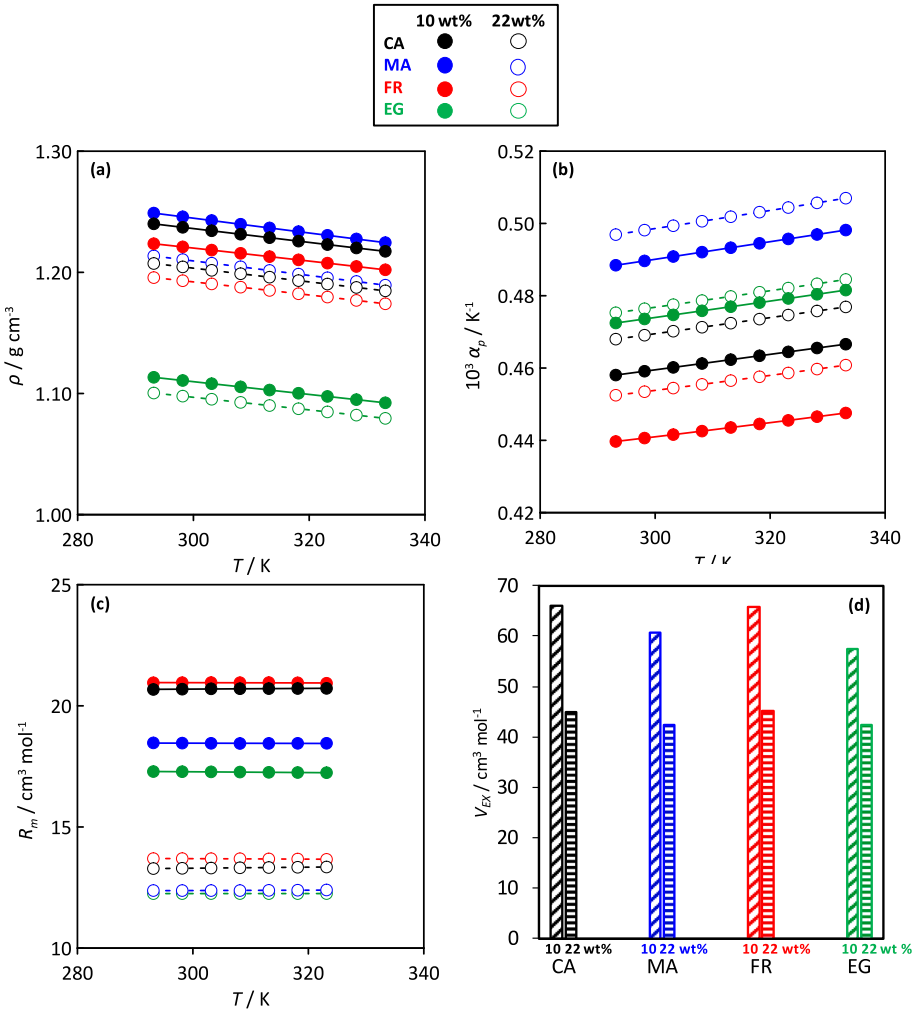

Fig. 5. CC:{CA, MA, FR, EG} 1:1 DESs with different water content reporting (a) density, ρ, (b) thermal expansion coefficient, α_p, (c) molar refraction, R_m, and (d) excluded volume, V_{EX}. Values in panel d are reported at 298.15 K.

water molecules initially occupying interstitial sites within the DESs structure before forming extended hydrogen-bonded networks that compete with the original DESs interactions.

3.5. Electronic structure and optical properties

The molar refraction data, Fig. 5c, provide insights into the electronic polarizability and the local electronic environment around the molecules. The systematic changes in molar refraction with water content reflect alterations in the electron density distribution and the strength of intermolecular interactions. These changes can be analyzed in terms of the electron donor-acceptor interactions between water molecules and the DESs components. The polarizability measurements at 298.15 K, Fig. 6, reveal how the electronic response of these systems changes with water addition. The variations in polarizability correlate with changes in the hydrogen bonding strength and can help explain the observed variations in other properties such as viscosity and conductivity. High polarizability systems tend to have stronger intermolecular interactions due to enhanced dispersion forces, which can contribute to the overall stability of the DESs structure.

3.6. Molecular-level interpretation and structural evolution

The reported thermophysical property measurements allow the development of an hypothetical molecular-level model on how water molecules integration affects the DESs structure for the considered

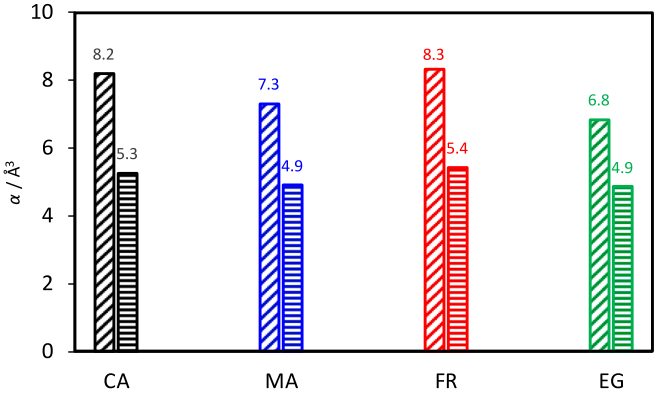

Fig. 6. CC:{CA, MA, FR, EG} 1:1 DESs with different water content reporting polarizability, α, at 298.15 K.

molecules. At low water concentrations (2 wt%), water molecules likely occupy specific binding sites within the existing DESs structure, potentially bridging between different ionic species or filling interstitial spaces. This integration can lead to either stabilization or destabilization of the original structure, depending on the compatibility between water's hydrogen bonding preferences and the existing network topology, but for the considered systems almost negligible disruption of hydrogen

bonding among DESs components.

At intermediate water concentrations (10 wt%), competition begins to emerge between the original DESs hydrogen bonding network and water-mediated interactions. The formation of water clusters or extended water networks becomes thermodynamically favorable, leading to a gradual reorganization of the molecular structure. This transition is reflected in the non-linear property changes observed across most measured parameters.

At high water concentrations (22 wt%), the system approaches a regime where water becomes the dominant component of the hydrogen bonding network, with the original DESs components becoming increasingly solvated species. This transition is accompanied by dramatic changes in transport properties, being especially relevant those for viscosity, and suggests a fundamental change in the nature of the liquid structure from a DES-like to a more conventional aqueous solution-like behavior. This behavior is summarized in Fig. 7.

The structural interpretations proposed herein—such as the initial occupation of interstitial voids by water molecules, the progressive formation of hydrogen-bonded water clusters, and the solvation effects around ionic species—are derived from observed changes in bulk thermophysical properties including viscosity, electrical conductivity, molar volume, and polarizability. While these interpretations are qualitative, they are grounded in well-established trends and corroborated by prior studies that similarly inferred molecular-level rearrangements from macroscopic measurements. For instance, variations in viscosity and excess molar volume in hydrated DESs could be directly correlated with the evolution of water–DES interactions and the formation of hydrogen bond-disrupted microdomains [22]. Likewise, macroscopic polarity and density trends reflect the presence of segregated water environments in DES systems, reinforcing the notion of localized structuring without requiring direct spectroscopic evidence [37]. Furthermore, molecular dynamics studies have confirmed that water in hydrated choline chloride-based DESs initially integrates into the DES hydrogen bond network, then progressively forms clusters as the water content increases—providing theoretical support for the assumptions made in this work [38].

Although spectroscopic techniques such as FTIR or Raman would provide direct insight into the hydrogen bonding motifs and solvation structures, the goal of this study was to build a thermophysical understanding of hydration effects across diverse HBD systems. Given the reproducibility, internal consistency, and temperature dependence of the measured properties, the molecular-level hypotheses presented serve as a physically reasonable framework to interpret the trends observed. Future studies using complementary spectroscopic or modeling tools will be essential to validate and refine these microscopic descriptions.

3.7. Thermodynamic stability and phase behavior considerations

The observed property trends also provide insights into the thermodynamic stability of these aqueous DESs systems. The smooth, continuous changes in most properties with water content suggest single-phase behavior across the investigated composition range. However, the non-linear relationships and the presence of apparent optimization points for certain properties suggest the existence of specific water-to-DESs ratios where particular molecular arrangements are favored. The temperature dependence of the considered properties provides information about the enthalpic and entropic contributions to the thermodynamic stability. Systems showing strong temperature dependence (high fragility, large thermal expansion coefficients) indicate that entropic effects dominate, while systems with weaker temperature dependence suggest enthalpic stabilization through strong intermolecular interactions.

3.8. Implications for molecular design and optimization

The structure-property relationships revealed in this study provide valuable guidelines for the rational design of aqueous DESs systems with tailored properties, especially for dynamic ones such as viscosity which are far from optimal from the industrial viewpoint for neat DES, both in terms of large values hindering efficient heat and/or mass transfer operations. The observation that CC:EG systems show the most predictable and systematic responses to water addition suggests that hydrogen bond donors with simple, flexible structures are optimal for applications requiring controlled property tuning through water addition. The complex behavior exhibited by the CC:CA system, while challenging for property prediction, also suggests opportunities for creating systems with unique, non-additive properties that could be valuable for

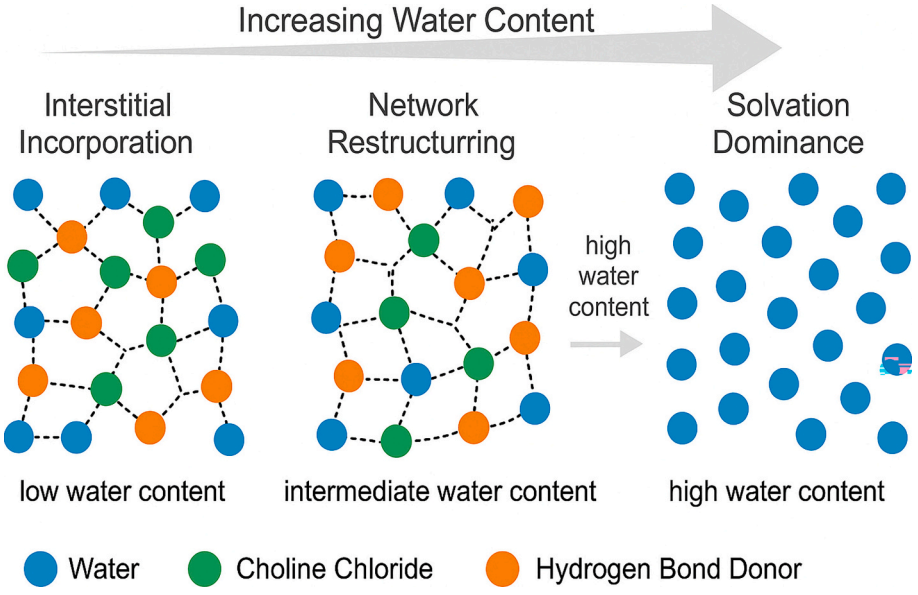

Fig. 7. Schematic representation of water integration into deep eutectic solvents (DESs) with increasing water content. Three hydration regimes are depicted: (i) Interstitial Incorporation—water molecules occupy voids within the DES hydrogen bonding network without major disruption; (ii) Network Restructuring—competition between water–DES and DES–DES hydrogen bonds leads to rearrangement of the structure; and (iii) Solvation Dominance—water becomes the continuous phase, and DES components act as solvated species. Color code: blue = water; green = choline chloride; orange = hydrogen bond donor.

specialized applications. The ability to create systems with high thermal stability while maintaining ionic conductivity, as demonstrated by the high *B* parameters coupled with reasonable conductivity values, opens possibilities for high-temperature electrochemical applications. The identification of optimal water concentrations for specific property combinations provides a framework for application-specific DESs design. The balance between reduced viscosity and maintained ionic conductivity at intermediate water concentrations makes these systems particularly attractive for electrochemical applications where both ion transport and manageable viscosity are critical requirements. To better contextualize the applicability of the investigated DESs systems in industrial settings, Table 3 compares the measured viscosity and electrical conductivity values at 22 wt% water and 298.15 K with common benchmark thresholds for electrochemical and process fluid applications (e.g., $\eta < 50$ mPa·s and $\sigma > 1$ mS/cm) [39], [40]. For benchmarking purposes, the well-studied CC:UREA (1:2) system with 24.5 wt% water content was also included. As shown in Table 3, CC:UR meets both industrial targets for viscosity and conductivity ($\eta = 2.30$ mPa·s; $\sigma = 77.97$ mS/cm), serving as a valuable reference to contextualize the performance of the novel systems studied in this work. Notably, all systems exceeded the conductivity threshold, confirming that moderate hydration significantly enhances ionic mobility across DESs types. However, only the ChCl:EG system met both viscosity and conductivity criteria simultaneously, positioning it as the most technically versatile for use in flowable electrochemical devices or thermal transport systems. The ChCl:FR system also displayed excellent conductivity, and while its viscosity slightly exceeds the target threshold, it remains within a processable range—suggesting it could be a viable bio-based alternative where sustainability is prioritized. In contrast, ChCl:CA and ChCl:MA remain limited by their high viscosities, despite improved conductivity upon hydration. Likewise, while viscosity and conductivity trends suggest potential for electrochemical applications, direct measurements of the electrochemical stability window (ESW) are not available in this study and will be addressed in future work. Given the sensitivity of ESW to hydration, structural flexibility, and ion dissociation, such measurements are expected to complement the present property analysis and enhance predictive solvent design.

These findings demonstrate that controlled water addition offers a practical strategy for tailoring DESs to specific application windows and highlight the importance of balancing fluidity and ion transport for functional solvent design.

Table 3
Comparison of DESs performance (22 wt% water, 298.15 K) vs. target industrial fluid requirements for electrochemical applications. Viscosity, η, and electrical conductivity, σ. Data for CC:UREA (1:2) are obtained for reference purposes [41]. For CC:UR (1:2) 24.5 wt% water content.

DES System	η / mPa·s	σ / mS/cm	Benchmark Range	Performance Notes
CC:UR (1:2)	2.298	77.97	η < 50 mPa·s, σ > 1 mS/cm	Meets both η and σ thresholds
CC:CA (1:1)	570.9	8.640		High σ, but too viscous
CC:MA (1:1)	212.9	1.175		Meets σ, but viscosity remains too high
CC:FR (1:1)	62.07	11.100		Nearly acceptable η, excellent conductivity
CC:EG (1:1)	14.18	26.800		Meets both η and σ thresholds

4. Conclusions

This work presents a systematic investigation into the thermophysical behavior of hydrated choline chloride-based deep eutectic solvents (DESs) formed with four structurally distinct hydrogen bond donors: citric acid, malic acid, fructose, and ethylene glycol. By studying hydration at 2, 10, and 22 wt% water, we reveal how water modulates key fluid properties—including viscosity, conductivity, thermal behavior, and structural organization—across a wide temperature range.

The application of Vogel–Fulcher–Tammann modeling to viscosity data uncovered distinct relaxation mechanisms and transitions from fragile to strong liquid behavior, particularly in systems with bio-derived HBDs. Notably, the ChCl:CA system showed highly cooperative dynamics and structural rigidity, while ChCl:EG exhibited predictable, tunable behavior suitable for engineered fluid systems. Water addition consistently enhanced electrical conductivity and reduced viscosity, with the ChCl:EG and ChCl:FR systems approaching industrial targets for flowable, conductive solvents.

Derived thermodynamic properties such as activation energy, fragility index, excess molar volumes, and polarizability provided insight into molecular interactions and the evolution of liquid structure upon hydration. These findings offer clear structure–property relationships that enable rational design of DESs for application-specific needs.

Finally, by comparing experimental data against practical performance thresholds, we demonstrate the feasibility of using water as a tuning agent to achieve industrially relevant fluid properties. This work provides a foundation for the design of next-generation, sustainable solvents for use in electrochemistry, separation processes, and thermal management.

CRediT authorship contribution statement

Rafael Alcalde: Writing – review & editing, Writing – original draft, Visualization, Validation, Methodology, Investigation, Formal analysis, Data curation. **Sergio de-la-Huerta-Sainz:** Writing – review & editing, Writing – original draft, Visualization, Validation, Methodology, Investigation, Formal analysis, Data curation, Conceptualization. **Valentin Diez-Cabanes:** Writing – review & editing, Writing – original draft, Visualization, Validation, Investigation, Formal analysis, Data curation, Conceptualization. **María A. Escobedo-Monge:** Writing – review & editing, Writing – original draft, Visualization, Validation, Investigation, Formal analysis, Data curation, Conceptualization. **Jose.L. Trenzado:** Writing – review & editing, Writing – original draft, Visualization, Validation, Supervision, Methodology, Investigation, Formal analysis, Data curation, Conceptualization. **Mert Atilhan:** Writing – review & editing, Writing – original draft, Visualization, Validation, Supervision, Methodology, Investigation, Formal analysis, Data curation, Conceptualization. **Alfredo Bol:** Writing – review & editing, Writing – original draft, Visualization, Validation, Supervision, Methodology, Investigation, Formal analysis, Data curation, Conceptualization. **Santiago Aparicio:** Writing – review & editing, Writing – original draft, Visualization, Validation, Supervision, Software, Resources, Project administration, Methodology, Investigation, Funding acquisition, Formal analysis, Data curation, Conceptualization.

Declaration of competing interest

The authors declare that they have no known competing financial interests or personal relationships that could have appeared to influence the work reported in this paper.

Acknowledgements

This research was funded by European Union (Horizon 2020 program, project WORLD: H2020-MSCA-RISE-2019-WORLD-GA-873005), and Agencia Estatal de Investigación (Project NADESforPFAS: PID2022-142405OB-I00). The statements made herein are solely the responsibility of the authors. The authors declare no competing interests.

Appendix A. Supplementary data

Viscosity data (Table S1); Density data (Table S2); thermal expansion

coefficient (Table S3); electric conductivity data (Table S4); thermal conductivity data (Table S5); polarizability data (Table S6); Procedure for calculating free volume; free volume data (Table S7); Fig. S1, results of VFT fits for experimental viscosity data.

Data availability

Data will be made available on request.

References

[1] V. Hessel, N.N. Tran, M.R. Asrami, Q.D. Tran, N. van Duc Long, M. Escribá-Gelonch, J. Osorio-Tejada, S. Linke, K. Sundmacher, Green Chem. 24 (2022) 410–437.

[2] P. Shah, S. Parikh, M. Shah, S. Dharaskar, A holistic review on application of green solvents and replacement study for conventional solvents, Biomass Convers. Biorefinery 12 (2021) 1985–1999.

[3] A. Prabhune, R. Dey, Green and sustainable solvents of the future: Deep eutectic solvents, J. Mol. Liq. 379 (2023) 121676.

[4] D. Yu, D. Jiang, Z. Xue, T. Mu, Deep eutectic solvents as green solvents for materials preparation, Green Chem. 26 (2024) 7478–7507.

[5] A. Azzouz, M. Hayyan, Are deep eutectic solvents biodegradable? Process. Saf. Environ. Prot. 176 (2023) 1021–1025.

[6] J. Afonso, A. Mezzetta, I.M. Marrucho, L. Guazzelli, History repeats itself again: Will the mistakes of the past for ILs be repeated for DESs ? From being considered ionic liquids to becoming their alternative: the unbalanced turn of deep eutectic solvents, Green Chem. 25 (2023) 59–105.

[7] B.B. Hansen, S. Spittle, B. Chen, D. Poe, Y. Zhang, J.M. Klein, A. Horton, L. Adhikari, T. Zelovich, B.W. Doherty, B. Gurkan, E.J. Maginn, A. Ragauskas, M. Dadmun, T.A. Zawodzinski, G.A. Baker, M.E. Tuckerman, R.F. Savinell, J. R. Sangoro, Deep Eutectic Solvents: A Review of Fundamentals and Applications, Chem. Rev. 121 (2021) 1232–1285.

[8] F. Xang, Q. Zheng, H. Tan, Z. Wang, Insight into the role of hydrogen bond donor in deep eutectic solvents, J. Mol. Liq. 399 (2024) 124332.

[9] A. Van Den Bruinhorst, M. Costa Gomes, Is there depth to eutectic solvents?, Current Opinion in Green and Sustainable, Chemistry 37 (2022) 100659.

[10] D.O. Abranches, L.P. Silva, M.A.R. Martins, S.P. Pinho, Understanding the Formation of Deep Eutectic Solvents: Betaine as a Universal Hydrogen Bond Acceptor, ChemSusChem 13 (2020) 4916–4921.

[11] Y. Chen, Z. Yu, Low-melting mixture solvents: extension of deep eutectic solvents and ionic liquids for broadening green solvents and green chemistry, Green Chem. Eng. (2023), https://doi.org/10.1016/j.gce.2023.11.001.

[12] Y. Chen, Z. Yu, Low-melting mixture solvents: extension of deep eutectic solvents and ionic liquids for broadening green solvents and green chemistry, Green Chem. Eng. 5 (2024) 409–417.

[13] T. El-Achkar, H. Greige-Gerges, S. Fourmentin, Basics and properties of deep eutectic solvents: a review, Environ. Chem. Lett. 19 (2021) 3397–3408.

[14] D.O. Abranches, J.A.P. Coutinho, Type V deep eutectic solvents: Design and applications, Curr. OP. Green Sus. Chem. 35 (2022) 100612.

[15] T. Juric, D. Uka, B.B. Holló, B. Jóvic, B. Kordíc, B.M. Popovíc, Comprehensive physicochemical evaluation of choline chloride-based natural deep eutectic solvents, J. Mol. Liq. 343 (2021) 116968.

[16] L. Schuh, M. Reginato, I. Florencio, L. Falcao, L. Boron, E. Fortes-Gris, V. Mello, S. N. Bao, From Nature to Innovation: The Uncharted Potential of Natural Deep Eutectic Solvents, Molecules 28 (2023) 7653.

[17] K. Wu, J. Ren, Q. Wang, M. Nuerjiang, X. Xia, C. Bian, Research Progress on the Preparation and Action Mechanism of Natural Deep Eutectic Solvents and Their Application in Food, Foods 11 (2022) 3528.

[18] N.P.E. Hikmawanti, D. Ramadon, I. Jantan, A. Munim, Natural Deep Eutectic Solvents (NADES): Phytochemical Extraction Performance Enhancer for Pharmaceutical and Nutraceutical Product Development, Plants 10 (2021) 2091.

[19] K. Nowacki, M. Wysokowski, M. Golinski, Synthesis and characterization of betaine-based natural deep eutectic solvents for electrochemical application, J. Mol. Liq. 424 (2025) 127071.

[20] M.H. Zainal-Abidin, M. Hayyan, W.F. Wang, Hydrophobic deep eutectic solvents: Current progress and future directions, J. Ind. Eng. Chem. 97 (2021) 142–162.

[21] F.M. Fuad, M.M. Nadzir, A.H. Kamaruddin, Hydrophilic natural deep eutectic solvent : A review on physicochemical properties and extractability of bioactive compounds, J. Mol. Liq. 339 (2021) 116923.

[22] H. Kivela, M. Salomaki, P. Vainikka, E. Makila, F. Poletti, S. Ruggeri, F. Terzi, J. Lukkari, Effect of Water on a Hydrophobic Deep Eutectic Solvent, J. Phys. Chem. B 126 (2022) 513–527.

[23] M.N. Nolasco, S.N. Pedro, C. Vilela, P.D. Paz, P. Ribeiro-Claro, S. Rudic, S. F. Parker, M.G. Freire, A.J.D. Silvestre, Water in Deep Eutectic Solvents: New Insights From Inelastic Neutron Scattering Spectroscopy, Front. Phys. 10 (2022), https://doi.org/10.3389/fphy.2022.834571.

[24] R. Ninayan, A.S. Levshakova, E.M. Khairullina, O.S. Veza, I.I. Tumkin, A. Ostendorf, L.S. Lagunov, A.A. Manshina, A.Y. Shishov, Water-induced changes in choline chloride-carboxylic acid deep eutectic solvents properties, Coll. Surf. A: Phys. Chem. Eng. Asp. 679 (2023) 132543.

[25] D. Peng, Z. Yu, A. Alhadid, M. Minceva, Modeling the Viscosity of ChCl-Based Deep Eutectic Solvents and Their Mixtures with Water, Ind. Eng. Chem. Res. 63 (2024) 1623–1633.

[26] M. Mohan, K.D. Jetti, M.D. Smith, O.N. Demerdash, M.K. Kidder, J.C. Smith, Accurate Machine Learning for Predicting the Viscosities of Deep Eutectic Solvents, J. Chem. Theor. Comput. 20 (2024) 3911–3926.

[27] F. Lin, Z. Zuo, B. Cao, H. Wang, L. Lu, X. Lu, Y. Zhu, X. Ji, A Comprehensive Study of Density, Viscosity, and Electrical Conductivity of Choline Halide-Based Eutectic Solvents in H_2O, J. Chem. Eng. Data 69 (2024) 4362–4376.

[28] A.S.D. Ferreira, R. Craveiro, A.R. Duarte, S. Barreiros, E.J. Cabrita, A. Paiva, Effect of water on the structure and dynamics of choline chloride/glycerol eutectic systems, J. Mol. Liq. 342 (2021) 117463.

[29] S. Rozas, C. Benito, R. Alcalde, M. Atilhan, S. Aparicio, Insights on the water effect on deep eutectic solvents properties and structuring: The archetypical case of choline chloride + ethylene glycol, J. Mol. Liq. 344 (2021) 117717.

[30] R. Alcalde, N. Aguilar, M.A. Escobedo, J.L. Trenzado, M. Atilhan, A. Bol, S. Aparicio, On the properties of water in betaine – based Deep Eutectic Solvents, J. Mol. Liq. 406 (2024) 124871.

[31] Y. Zuo, X. Chen, N. Wei, J. Tong, Effect of water or ethanol on the excess properties of deep eutectic solvents (tetrabutylammonium bromide + formic acid/propionic acid), J. Mol. Liq. 383 (2023) 122034.

[32] O. Sethi, M. Singh, T.S. Kang, A.K. Sood, Volumetric and compressibility studies on aqueous mixtures of deep eutectic solvents based on choline chloride and carboxylic acids at different temperatures: Experimental, theoretical and computational approach, J. Mol. Liq. 340 (2021) 117212.

[33] Y. Dai, J. VAN Spronsen, G.J. Witkamp, R. Verpoorte, Y.H. Choi, Natural deep eutectic solvents as new potential media for green technology, Anal. Chem. Acta 766 (2013) 61–68.

[34] H.J. Hayler, S. Perkin, The eutectic point in choline chloride and ethylene glycol mixtures, Chem. Commun. 58 (2022) 12728–12731.

[35] A. Paiva, R. Craveiro, I. Aroso, M. Martins, R.L. Reis, A.R.C. Duarte, Natural deep eutectic solvents – solvents for the 21st century, ACS Sustain. Chem. Eng. 2 (2014) 1063–1071.

[36] C.A. Angell, N. Byrne, J.-P. Belieres, Parallel developments in aprotic and protic ionic liquids: physical chemistry and applications, Acc. Chem. Res. 40 (2007) 1228–1236.

[37] Y. Dai, G.J. Witkamp, R. Verpoorte, Y.H. Choi, Tailoring properties of natural deep eutectic solvents with water to facilitate their applications, Food Chem. 187 (2015) 14–19.

[38] R. Contreras, L. Lodeiro, N. Rozas, R. Ormazabal, On the role of water in the hydrogen bond network in DESs : an ab initio molecular dynamics and quantum mechanical study on the urea–betaine system, Phys. Chem. Chem. Phys. 23 (2021) 1994–2004.

[39] K. Xu, Electrolytes for lithium and lithium-ion batteries, Chem. Rev. 104 (2004) 4303–4418.

[40] D.R. MacFarlane, N. Tachikawa, M. Forsyth, J.M. Pringle, P.C. Howlett, G. D. Elliott, J. Davis, M. Watanabe, P. Simon, C.A. Angell, Energy applications of ionic liquids, Energy Environ. Sci. 7 (2014) 232–250.

[41] V. Agieinko, R. Buchner, Densities, viscosities, and electrical conductivities of pure anhydrous reline and its mixtures with water in the temperature range (293.15 to 338.15) K, J. Chem. Eng. Data 64 (2019) 4763–4774.